Research on Surface Subsidence Monitoring of Yanghuopan Coal Mine Based on SBAS-InSAR Technology

Yuhai Fan[*a, b, c1], Rui Gao [d], Huaidonga Bai [a]

[a*]China Coal Aerial Survey and Remote Sensing Bureau, Xi'an 710054, Shaanxi, China;
[b]Yulin University,Yulin,Shaanxi 719000,China;
[c]Yulin Tongda Mingtai Geological Technology Co., LTD,Shaanxi 719000,China;
[d]Shenmu Vocational & Technical College, Shaanxi 719300, China

ABSTRACT

The mining of coal resources in Yanghupan has caused a large area of land surface subsidence within the mining area, which has seriously affected the production and life of local people.In this paper, multi-view Sentinel-1A data from Yanghuopan Coal mine was selected and SBAS-InSAR technology was adopted to conduct fine monitoring of the mining area through multi-time series SAR images (October 2017 - May 2019), so as to realize high-precision monitoring and early warning of mining area safety production.The monitoring results show that there are four large subsidence centers in the eastern part of Yanghupan mining area, with the maximum shape variable of -85mm/y and the cumulative shape variable of -128mm. Subsidence is still occurring in the surface deformation area found in the mining area.

Keywords: SBAS-InSAR, surface subsidence, deformation monitoring, Yanghuopan Coal mine

1. INTRODUCTION

Yanghuopan Coal Mine is located in Dianta Town, Shenmu County, Shaanxi Province. It belongs to Shenfu mining area of Jurassic coal field in northern Shaanxi Province. It covers an area of 26.9176km^2 and is delimit by the line of 10 turning points[1].The mining of coal resources in Yanghuopan leads to a large area of land surface settlement within the mining area, which seriously affects the production and life of local people [2-3].It is an important purpose to pay attention to the surface subsidence in mining area and realize the geological safety and sustainable development of mining area. In this paper, multi-view Sentinel-1A data from Yanghuopan Coal mine was selected and SBAS-InSAR technology was adopted to conduct fine monitoring of the mining area through multi-time series SAR images (October 2017 - May 2019), so as to realize high-precision monitoring and early warning of mining area safety production.

2. OVERVIEW OF THE STUDY AREA

Most of the surface of Yanghuopan Coal mine is covered by Quaternary and Neogene sediments, and only the bedrock is exposed along Huangyangchenggou and Dabantuchuan branch ditch. The strata of coal mine from old to new are: Upper Triassic Yongping Formation (T_3y), Lower Jurassic Fuxian Formation (J_1f), Middle Jurassic Yan 'an Formation (J_2y), Upper Neogene Baode Formation (N_2b) and Quaternary loess and river sediments. The coal mine is a monoclinal structure, no fault, magmatic rock found, the structure is very simple. The Yanan Formation of middle Jurassic system is the main coal-bearing stratum, and the four coal seams with mining value are 2^{-2}, 3^{-1}, 4^{-3} and 5^{-1}. The whole mine is set at two levels, one level is set at 3^{-1} coal, the other level is set at 5^{-1} coal, and auxiliary levels are set in 2^{-2} coal and 4^{-3} coal seams. The coal mining method is one full height comprehensive mechanized coal mining.

3. DATA SOURCE SELECTION

The SAR image data contains deformation phase information, and the three-dimensional and deformation information of the surface can be obtained from the phase information by using InSAR technology [4-6]. The data used in this study mainly

[1*]170269854@qq.com

The International Conference Optoelectronic Information and Optical Engineering (OIOE2024), edited by Yang Yue, Lu Leng, Proc. of SPIE Vol. 13513, 135134B · © 2025 SPIE · 0277-786X · © The Authors.
 · doi: 10.1117/12.3056698

include Sentinel-1 satellite image (resolution: 20m), precision satellite orbit data (POD, accuracy: 5cm) and ALOS Global Digital Surface Model(AW3d30) data (resolution: 30m).

3.1 Sentinel-1 satellite data

The Sentinel-1 satellite is equipped with the European Polar Orbit C-band radar imaging System, which has the ability to observe any location around the world with a time delay of better than one hour. Sentinel-1 satellite data has the characteristics of short return period, large monitoring range and multiple working modes, and has been widely used in many disciplines and fields, such as environmental monitoring, polar research, agricultural monitoring, earth science, disaster risk monitoring and emergency response. This time, the Sentinel-1A satellite orbital SAR images from October 2017 to May 2019 were adopted, with a resolution of 5m×20m and a mapping resolution of 20m.

3.2 Sentinel-1 precision orbit data

Satellite orbit data, as an important parameter file, contains information such as position, attitude and direction of satellite operation, and plays a vital role in radar image signal processing. This precision track data adopts POD precision track data released 21 days after imaging, and the positioning accuracy can reach 5cm, and then the data is processed by SBAS-InSAR.

3.3 DEM Data

In deformation monitoring, in order to remove the terrain phase in the interference phase, high-precision DEM data is also needed in the process of processing for registration, removal of terrain phase and other operations. The latest AW3D DEM was selected as the auxiliary data. AW3D30, generated by PRISM on the Japanese Earth observation satellite ALOS, covers the global land area between 82°N and 82°S with a horizontal resolution of 30 m (1 arcsecond) and an elevation accuracy of 5 m, making it the most accurate 3D map in the world. This time, the DEM data is AW3D DEM data, and the grid interval is 30m.

4. SURFACE DEFORMATION MONITORING

This surface deformation monitoring uses SBAS-InSAR technology, which uses multi-view SAR image data to select appropriate spatial baseline, time baseline and Doppler centroid difference to form an optimal connection map, and finally realizes MM-level precision monitoring through a series of operations such as interferogram generation, filtering and atmospheric phase separation.

4.1 Data Processing

The collected Sentinel-1 SAR data, orbit precision files and DEM data were used for SBAS-InSAR data processing. SBAS-InSAR data processing is completed in ENVI SARscape software, which can be divided into: data preparation, connection map generation, differential interferogram generation, coherent point target selection, deformation calculation, atmospheric phase removal, geocoding and other steps.

In this setting, the time baseline was 4% and the space baseline was 120 days. A total of 392 pairs of interference image pairs were obtained in the interference processing stage, and the average intensity image was obtained based on the spatiotemporal baseline.

4.2 Settlement result

The SBAS-InSAR method combines as many small data sets as possible according to a small time/space baseline threshold through the multi-master image strategy. In the deformation solving process, SAR data sets separated by larger baselines can be connected by the singular value decomposition method, a single point deformation phase equation can be established, and the deformation rate and its time series cumulative shape variables can be obtained (Figure 1). The surface deformation map was statistically analyzed with GIS tools, and the area statistics of different subsidence areas were obtained (Table 1). As can be seen from Table 1, during the period from October 2017 to May 2019, a total of 25.86km^2 of land had land subsidence disaster, accounting for 96.4% of the total area of the study area. The land area with obvious subsidence and subsidence of more than 20mm was 3.7km^2, accounting for 13.79% of the total area. The area with the most serious surface subsidence (subsidence of more than 100mm) has an area of 0.08km^2. Most of them are located in the eastern part of the mining area.

It can be seen from Figure 1 that the surface subsidence of Yanghuopan Coal mine is mainly located in four areas A, B, C and D in the eastern part of the mining area. The region of point A shows a large subsidence (that is, away from the satellite direction) and the subsidence range is the largest, and the average annual maximum subsidence rate is -85mm/y. The maximum sedimentation rate at point B is -63mm/y, and the A and B regions tend to be connected into sheets. The maximum sedimentation rate at point C is -50mm/y. The maximum sedimentation rate at point D is -60mm/y.

Table 1 Statistical table of surface deformation in mining area

Number	Shape variable/ mm	Settling area（m²）	proportion（%）	Number	Shape variable/ mm	Settling area（m²）	proportion（%）
1	＞0	394987	1.47	5	-50～-80	727154	2.71
2	0	566734	2.11	6	-80～-100	227825	0.85
3	-1～-20	22160850	82.63	7	-100～-120	81154	0.3
4	-20～-50	2654912	9.9	8	＞-120	6740	0.03

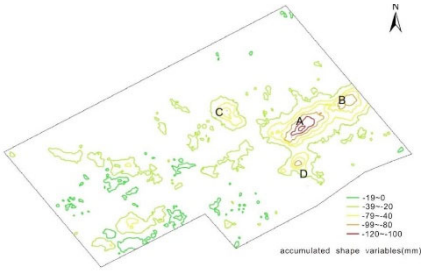

Figure. 1 Contour map of accumulated shape variables in mining area

4.3 Analysis of settlement results

In order to more intuitively represent the spatial distribution of settlement region, A three-dimensional visualization diagram of settlement superposition is generated in ArcScene software (Figure 2). It can be seen that in the settlement region of the mining area, the settlement trend is obvious at points A, B and C, and there is an obvious settlement funnel at point A and point B, and there is an obvious linking trend. The settlement of C and D points is small. At the same time, it is also clear that different areas have different degrees of subsidence.

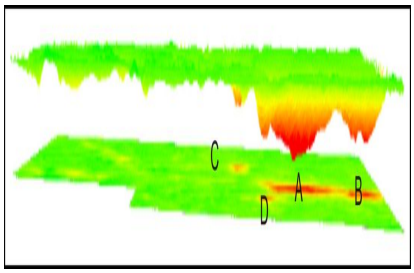

Figure. 2 Three-dimensional visualization of settlement superposition in mining area

According to the changes of sedimentation amount at points A, B, C and D in the time series (Figure 3), as time goes on, the sedimentation amount of the two typical sedimentation zones at points A and B gradually increases, while the sedimentation of the two sedimentation zones at points C and D slows down and basically becomes stable. Obviously, the settling velocity of point A is greater than that of point B, and the settling range of point A can be seen to be greater than that of point B. The sedimentation rate at point C and D gradually slows down, indicating that point C and D are currently stable in the region.

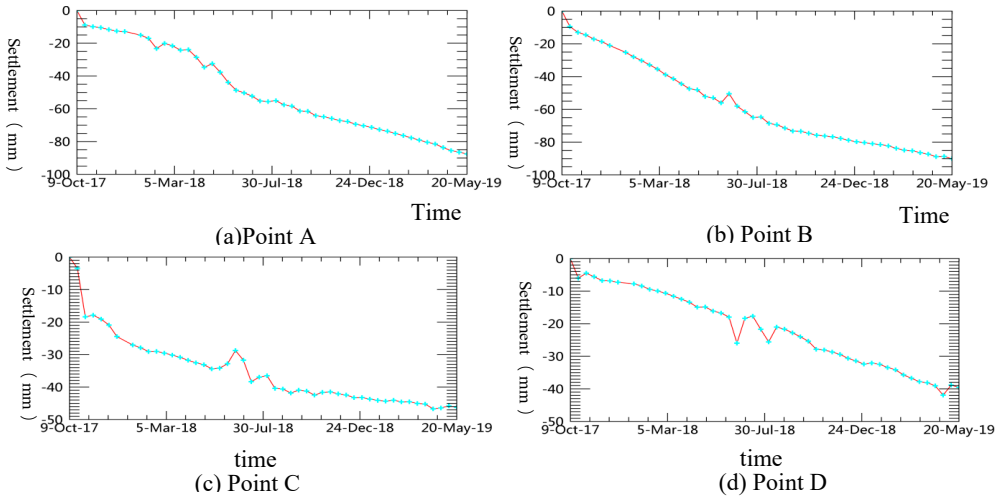

Figure. 3 Settlement of time series

5. FIELD VERIFICATION OF GROUND SETTLEMENT DETECTION

In order to evaluate the accuracy and validity of the InSAR monitoring results, field leveling was carried out in the working area. A total of 25 ground points were deployed and field measurements were carried out in three phases using COSA ground control measurements. The height of this survey adopts 1985 national height datum; The line elevation control survey is carried out by the fourth level survey, and the final adjustment calculation is carried out by the COSA ground control survey data processing system.

The elevation control network is composed of two closed rings: Line 1: DD1-JK1-JK2-JK3-JK4-JK5-JK6-JK7-JK8-D6; Line 2: D6-JK23-JK20-JK19-JK21-JK22-DD1; Line 3: DD1-JK9-JK10-JK11-JK12-JK13-JK14-JK15-JK16-JK17-JK18.

Two third grade level points (DD1, D6) were jointly measured, and the known level points were taken as the starting point. The height closure difference of each closed ring meets the requirements of National Standard for Third and fourth Level Surveying (GB_T12898-2009). When calculating the adjustment of elevation control, all the fourth grade level points of the whole network are unified adjustment calculation, and the fourth grade level measurement results of each point are obtained (Table 2).

According to the leveling monitoring data of the third phase (Figure 4), settlement deformation exists in most areas of the mining area, among which four points in the first two measurement data have a large settlement, reaching the maximum of -761mm (JK16 point). In the comparison of the second and third measurement data, these four points have the largest uplift, reaching 671.8mm. The settlement of other points is about 20mm. It can be seen from the superposition diagram of leveling points and cumulative shape variables that the settlement position of leveling is consistent with the InSAR monitoring settlement area.

Table 2 Leveling difference table

Dot mark	The difference between the second and first levels(mm)	The difference between the third and second levels(mm)	Dot mark	The difference between the second and first levels(mm)	The difference between the third and second levels(mm)
DD1	0	0	JK20	-27.5	-30.4
D6	0	0	JK21	-18	-60.3
JK1	-22.4	-9.6	JK9	-345.8	296.7
JK2	-21	-22.2	JK10	-657.7	607.7
JK3	-10.9	-50.3	JK11	-659.1	607.1
JK4	-21	-44.1	JK12	-23.5	-28.8

Dot mark	The difference between the second and first levels(mm)	The difference between the third and second levels(mm)	Dot mark	The difference between the second and first levels(mm)	The difference between the third and second levels(mm)
JK5	-16.9	-56.2	JK13	-15	-38.5
JK6	-17.8	-54	JK14	-16.8	-57.1
JK7	-14.7	-61.4	JK15	-18.8	-53.9
JK8	-33.8	-53.3	JK16	-761.5	671.8
JK23	-14.6	-14.5	JK17	-11.9	-78.1
JK22	-18.8	-5.6	JK18	-22.8	-66.3
JK19	-26.5	-31.9			

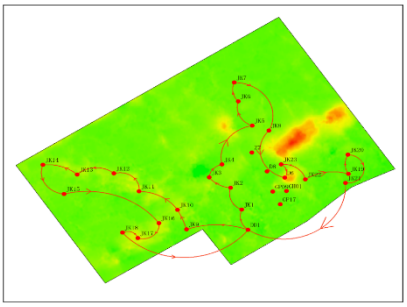

Figure.4 Stacking diagram of leveling and cumulative shape variables

6. CONCLUSION

(1) From October 2017 to May 2019, subsidence was still occurring within the surface deformation range found in Yanghuopan Coal Mine; There are four large subsidence centers in Yanglupan mine area, with the maximum shape variable of -85mm/y and the cumulative shape variable of -128mm. The occurrence of geological disasters is A process of slow accumulation to eruption. It is suggested to continue to carry out deformation monitoring in the study area, especially in the A and B areas, so as to avoid large-scale surface deformation.

(2) InSAR technology can effectively obtain surface deformation information of mining area, provide comprehensive deformation information for comprehensive settlement treatment of mining area, give early warning before disasters occur, take protective measures in advance, and reduce losses.

REFERENCES

[1] Wand N., Li H. T., Cui S., Wand H., Zhu Z. R., Zuo X. F. and Zhao Z., Impact from underground coal fire on coal structure in Yanghuopan Mine Area ,Shenmu , Coal geology of China, 32(4):1-5,(2020).

[2] Fan D.Q., Qiu Y., Sun W. B., Zhao X. S., Mai X. M., Hu Y. W. , Evaluating ecological environment based on remote sensing ecological index in Shenfu mining area, Surveying and mapping bulletin, (7):23-28, (2021).

[3] Chen F. Y., Guo Z. H., Zhang Y. H., Xu K.L., Jiang X.G., Evaluation of ecological environment quality of northern Shaanxi mining area based on remote sensing and GIS technology-taking Yanghuopan mining area as an example , China Coal, 46(6):45-51(2020).

[4] Yin S.W., The road subsidence monitoring based on coherent target DInSAR technique in South of China, Zhengzhou: Master's thesis of PLA Information Engineering University, (2010).

[5] Deng Y. S., Research on surface subsidence monitoring of coal mining area based on D-InSAR technology, Master's thesis, East China University of Science and Technology, (2017).

[6] Guo, S.C., Hou, H.P., Zhang, S.L., Xu, Y.Q., Yang, Y.J.,Surface deformation monitoring of the mining area in Loess Plateau based on D-InSAR, Science of Surveying and Mapping, 42(6):207-212(2017).